Article

Structure of the Monoclinic-Form Misfit-Layer Compound, (CaOH)CoO (0.57822)

Masaaki Isobe, Mitsuko Onoda, Mitsuyuki Shizuya, Masahiko Tanaka, and Eiji Takayama-Muromachi

J. Am. Chem. Soc., **2007**, 129 (47), 14585-14596 • DOI: 10.1021/ja072052v

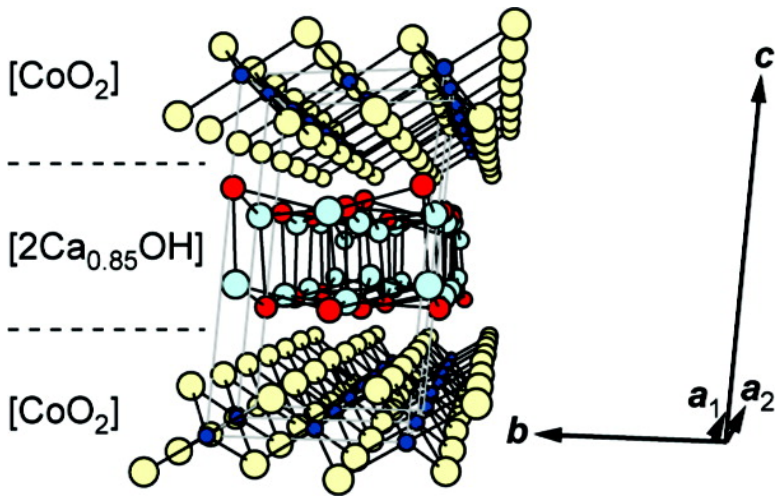

More About This Article

Additional resources and features associated with this article are available within the HTML version:

- Supporting Information
- Links to the 1 articles that cite this article, as of the time of this article download
- Access to high resolution figures
- Links to articles and content related to this article
- Copyright permission to reproduce figures and/or text from this article

View the Full Text HTML

J|A|C|S
ARTICLES
Published on Web 11/06/2007

Structure of the Monoclinic-Form Misfit-Layer Compound, $(Ca_{0.85}OH)_{2\alpha}CoO_2$ ($\alpha \approx 0.57822$)

Masaaki Isobe,* Mitsuko Onoda, Mitsuyuki Shizuya, Masahiko Tanaka, and Eiji Takayama-Muromachi

Contribution from the National Institute for Materials Science (NIMS), 1-1 Namiki, Tsukuba, Ibaraki 305-0044, Japan

Received March 23, 2007; E-mail: isobe.masaaki@nims.go.jp

Abstract: The incommensurate modulated crystal structure of the new misfit-layer calcium cobalt oxide $(Ca_{0.85}OH)_{2\alpha}CoO_2$ was investigated using a superspace-group formalism with synchrotron X-ray diffraction data. The compound is a kind of composite crystal that consists of two interpenetrating subsystems, $[CoO_2]_\infty$ layers containing triangular lattices formed by edge-sharing CoO_6 octahedra, separated from each other by $[2Ca_{0.85}OH]_\infty$ double-layered rock-salt-type slabs. Both the subsystems are monoclinic lattices with the unit cell parameters, $a_1 = 2.8180(4)$ Å, $b = 4.8938(6)$ Å, $c = 8.810(1)$ Å, $\alpha_0 = 95.75(3)°$, and $\alpha(=|\boldsymbol{q}|=a_1/a_2) = 0.57822(8)$, viz., $a_2 = 4.8736$ Å, with $Z = 2$. A possible superspace group is $C2/m(\alpha 10)s0-C2_1/m(\alpha^{-1}10)$ for the respective subsystems. The atomic positions deviate from the average positions of the fundamental structure due to the incommensurable periodic interaction between the subsystems. A significant structural modulation was found in the $[2Ca_{0.85}OH]$ subsystem, whereas the modulation in the $[CoO_2]$ subsystem is less than in $[2Ca_{0.85}OH]$, due to the tight bonding of the close-packed CoO_6 octahedra. The degree of modulation in the CoO_2 layers, i.e., the potential modulation, is almost the same as those of other compounds of the misfit-layer cobalt oxides. Flattened CoO_6 octahedra indicate hole doping into the CoO_2 layers. The $[2Ca_{0.85}OH]$ blocks act as the charge reservoir layers, and the defect Ca ions are presumably the source of the holes.

Introduction

Layered cobalt oxides have generated much interest recently with solid-state physicists and chemists because these materials are correlated electron materials exhibiting unusual electronic properties. The interest is focused, in particular, on the unconventional superconductivity observed below 5 K in hydrated $Na_{0.35}CoO_2 \cdot 1.3H_2O$.[1] This superconductivity is of great interest because of the unusual electron pairing, mediated due to the possible magnetic fluctuations.[2] Furthermore, there is also interest in the unusually large thermoelectric power coexisting with low electric resistivity in the layered cobalt oxides, such as $NaCo_2O_4$[3] and $Ca_3Co_4O_9$.[4] This effect is considered to originate from a large hidden entropy associated with spin frustration on the triangle lattice in the CoO_2 layer.

The structure of the cobalt oxides consists of layers of Co atoms, within an octahedral environment of oxygen atoms, arranged on a triangle lattice. The charge and spin correlation is found to occur mainly in the CoO_2 layers. The blocking layer, which consists of single or multiple atomic layers, interlinks between the CoO_2 layers, forming a series of cobalt oxide layers. It was suggested that the blocking layer could be replaced with different elements or structure blocks while keeping the framework of the CoO_2 block. Motivated by this hypothesis we searched for a new member to the layered cobalt oxide family. Recently, two new cobalt calcium hydroxides were synthesized for the first time using the solid-state reaction method at a high temperature and pressure.[5−7] These two new materials are $(CaOH)_{1.14}CoO_2$, which exhibits an orthorhombic lattice structure, and $(Ca_{0.85}OH)_{1.16}CoO_2$, which exhibits a monoclinic lattice structure, where the orthorhombic phase is a polytype of the monoclinic phase.

In this study we report on the crystal structure of the recently discovered compound, $(Ca_{0.85}OH)_{1.16}CoO_2$. The basic structure was initially studied using conventional X-ray and electron diffraction.[7] It was reported that the compound includes a double layered $Ca_{0.85}OH$ structure block as the blocking layer, situated between the CoO_2 layers in the structure. Some of the Ca sites are defective, resulting in a mixed-valence state for the Co ions. The two subsystems, $[CoO_2]$ and $[2Ca_{0.85}OH]$, have incommensurable periodicity along the *a*-axis resulting in a misfit-layer structure. Thus, we anticipate the crystal structure is being modulated due to the intersubsystem interaction. The structural modulation may affect carrier conduction through the potential modulation in the CoO_2 layer. It is, therefore, important to clarify

(1) Takada, K.; Sakurai, H.; Takayama-Muromachi, E.; Izumi, F.; Dilanian, R. A.; Sasaki, T. *Nature* **2003**, *422*, 53.
(2) Singh, D. J. *Phys. Rev. B* **2003**, *68*, 020503R.
(3) Terasaki, I.; Sasago, Y.; Uchinokura, K. *Phys. Rev. B* **1997**, *56*, R12685.
(4) Masset, A. C.; Michel, C.; Maignan, A.; Hervieu, M.; Toulemonde, O.; Studer, F.; Raveau, B.; Hejtmanek, J. *Phys. Rev. B* **2000**, *62*, 166.
(5) Shizuya, M.; Isobe, M.; Baba, Y.; Nagai, T.; Osada, M.; Kosuda, K.; Takenouchi, S.; Matsui, Y.; Takayama-Muromachi, E. *J. Solid State Chem.* **2007**, *180*, 248.
(6) Isobe, M.; Onoda, M.; Shizuya, M.; Tanaka, M.; Takayama-Muromachi, E. *J. Phys. Soc. Jpn.* **2007**, *76*, 014602.
(7) Shizuya, M.; Isobe, M.; Baba, Y.; Nagai, T.; Matsui, Y.; Takayama-Muromachi, E. *J. Solid State Chem.* **2006**, *179*, 3974.

the incommensurate modulated structure in detail, to better understand the observed physical properties.[7] However, other researchers have yet to report a structural analysis of the material. This is presumably because neutron diffraction experiments may be ineffective for the structural analysis. The neutron diffraction measurements are affected by the large bound incoherent scattering due to the hydrogen atoms found in the present compound.

In this study the modulated crystal structure of $(Ca_{0.85}OH)_{1.16}CoO_2$ was investigated in detail using the superspace-group approach. Data was obtained using a Debye−Scherrer-type synchrotron X-ray diffraction method, which is presently the best method one can employ to reduce the influences of the bound incoherent scattering and the strong preferred orientation due to the layered structure. From the analysis of the diffraction data we found that the compound has a unique structural modulation. The $Ca_{0.85}OH$ block, in particular, is strongly combined and interacts with the CoO_2 layer block. On the basis of these results the hole-doping level at the Co sites and the degree of the potential modulation in the CoO_2 layer was investigated further. In the following discussion the relationship between the hole-doping mechanism and the Ca defect, through the local structural modulation, is considered in detail.

Experimental Section

Sample Preparation. Polycrystalline monoclinic samples of $(Ca_{0.85}OH)_{1.16}CoO_2$ were prepared using the high-pressure solid-state reaction method. Starting reagents, Co_3O_4, CaO_2, CaO, and $Ca(OH)_2$, with an atomic molar ratio of Ca/Co/O/H = 1:1:3.333:1.167 were mixed using an agate mortar in a glove box filled with dry Ar gas. The mixture was sealed into a gold capsule and then heated in a flat-belt-type high-pressure apparatus under 6 GPa at 1200 °C for 1 h, followed by quenching to room temperature before releasing the pressure. The product, as grown, was washed in deionized water to remove the small amounts of unreacted $Ca(OH)_2$. The final product sample quality was checked using conventional X-ray diffraction. The sample was confirmed to be pure enough for a precise structure analysis. The atomic composition of the phase is $(Ca_{0.85}OH)_{1.16}CoO_2$, reported in a previous paper.[7]

Diffraction Measurement. Synchrotron X-ray diffraction data for the analysis of the crystal structure of the materials was obtained using a high-resolution powder diffractometer[8] installed at the BL15XU beam line of SPring-8 with Debye−Scherrer geometry, using a Ge(111) analyzer[9] and a YAP detector. Incident beams from an undulator were monochromatized to a wavelength of 0.8 Å, with inclined Si(111) double-crystal monochromators. The fine-particle powder sample was loaded into a quartz-glass capillary tube (inner diameter 0.5 mm) and was rotated at a speed of about 1.2 cps during the measurement. The diffraction data were collected at room temperature in a 2θ angle range, from 3° to 70°, in a step size of 0.005° and a counting time of 5 s per step.

Analysis Software. The synchrotron X-ray diffraction data were analyzed using the Rietveld-refinement software, PREMOS2k*i* and PREMOS91, designed by Yamamoto[10] for modulated structure analysis. Crystal structures were drawn using PRJMS. Interatomic distances were plotted using MODPLT. Restrictions of harmonic amplitudes of modulation functions were calculated using SPLPOS. These computer programs are included in the REMOS95.1 software package.[11]

Table 1. Assumed Four-Dimensional Superspace Groups for $(Ca_{0.85}OH)_{2\alpha}CoO_2$ ($\alpha = 0.57822$)

subsystem	1: $[CoO_2]_\infty$	2: $[2Ca_{0.85}OH]_\infty$
modulation vector, $\boldsymbol{q}^a$	$\alpha\boldsymbol{a}_1^*$	$\alpha^{-1}\boldsymbol{a}_2^*$
centering translation	1/2, 1/2, 0, 1/2	1/2, 1/2, 0, 1/2
symmetry operators	x, y, z, t	x, y, z, t
	$x, -y, -z, t+1/2$	$x+1/2, -y, -z, t$
	$-x, -y, -z, -t$	$-x, -y, -z, -t$
	$-x, y, z, -t+1/2$	$-x+1/2, y, z, -t$
symbol	$C2/m(\alpha 10)s0$	$C2_1/m(\alpha^{-1}10)$

[a] $\alpha = a_1/a_2$. $\boldsymbol{a}_1^*$ and $\boldsymbol{a}_2^*$ are unit reciprocal-lattice vectors along the a^*-axis for subsystem 1 and 2, respectively.

Structure Analysis

Superspace-Group Symmetry. Electron microscopy of $(Ca_{0.85}OH)_{1.16}CoO_2$ was performed in the original work.[7] The electron diffraction patterns clearly show that the sample is in an incommensurate phase that belongs to the class of composite crystals having a (3 + 1)-dimensional structure. The main reflection spots in the electron diffraction patterns were assigned by superimposition of two sets of monoclinic reciprocal lattices corresponding to the two subsystems, with common $\boldsymbol{b}^*$ and $\boldsymbol{c}^*$ ($b \approx 4.9$ Å, $c \approx 8.8$ Å, and $\alpha_0 = 95.7°$) unit vectors, and different $\boldsymbol{a}_1^*$ and $\boldsymbol{a}_2^*$ (unique axis, $a_1 \approx 2.8$ Å for the subsystem 1 and $a_2 \approx 4.9$ Å for the subsystem 2). Some weak satellite spots, due to incommensurate modulation resulting from the intersubsystem interaction, were observed along the $\boldsymbol{a}^*$-axis. Both the main and satellite reflections are systematically indexed by a set of four integers *hklm*, with a reciprocal-lattice vector $\boldsymbol{h}$ given by: $\boldsymbol{h} = h\boldsymbol{a}_1^* + k\boldsymbol{b}^* + l\boldsymbol{c}^* + m\boldsymbol{a}_2^*$, where $\boldsymbol{a}_2^* = \alpha\boldsymbol{a}_1^*$ ($\alpha \approx 0.578$: incommensurability).[12] The modulation wavevector, $\boldsymbol{q}$, is $\alpha\boldsymbol{a}_1^*$ for the subsystem 1 and $\alpha^{-1}\boldsymbol{a}_2^*$ for the subsystem 2.

Systematic extinctions were found: $h + k + m =$ odd is absent for the (*hklm*) reflections. This implies C-centering with a centering translation of (1/2,1/2,0,1/2). The extinction condition, $l =$ odd is absent for the (0*kl*0) reflections, was not observed. This implies a tentative centrosymmetric symbol, *C*2/*m*, or its lower-symmetry noncentrosymmetric symbols, *C*2 or *Cm*, for both the subsystems. The other extinction condition is found for a special subset of reflections: $m =$ odd and $h =$ odd are absent for the (*h*00*m*) reflections.[13] Therefore, for a centrosymmetric structure, the superspace group compatible with the Laue symmetry, and all the extinction conditions, is *C*2/*m*(α10)*s*0 for the subsystem 1. This symbol is equivalent to *B*2/*m*(00γ)*s*0 (No. 12.4) in Table 9.8.3.5 of ref 14. Corresponding symmetry operations, i.e., elements of the superspace group, are summarized in Table 1. Elements of the superspace group of the subsystem 2 was obtained by coordinate transformation in superspace with the following permutation matrix, $\mathbf{P}_\nu = (1,4)$ ($\nu = 2$: subsystem number). Thus, $C2_1/m(\alpha^{-1}10)$ is a suitable superspace-group symbol for subsystem 2. For a noncentrosymmetric structure the appropriate noncentrosymmetric superspace groups should be used, e.g., *C*2(α10)*s*, etc.

Determination of the Basic Structure. From electron diffraction data it was found that $(Ca_{0.85}OH)_{1.16}CoO_2$ has the

(8) Ikeda, T.; Nisawa, A.; Okui, M.; Yagi, N.; Yoshikawa, H.; Fukushima, S. *J. Synchrotron Rad.* **2003**, *10*, 424.
(9) Nisawa, A.; Okui, M.; Yagi, N.; Mizutani, T.; Yoshikawa, H.; Fukushima, S. *Nucl. Instrum. Methods Phys. Res., Sect. A* **2004**, *497*, 563.
(10) Yamamoto, A. *Acta Crystallogr., Sect. A* **1993**, *49*, 831; Yamamoto, A. *Acta Crystallogr., Sect. A* **1996**, *52*, 509.
(11) Yamamoto, A. http://www.nims.go.jp/aperiodic/yamamoto/index.html.
(12) Yamamoto, A. *Acta Crystallogr., Sect. A* **1982**, *38*, 87.
(13) This extinction was determined by excluding additional (forbidden) reflections due to stacking faults or multiple reflections from the observed electron diffraction patterns.
(14) Janssen, T.; Janner, A.; Looijenga-Vos, A.; de Wolff, P. M. In *International Tables for Crystallography*; Prince, E., Ed.; Kluwer: Dordrecht, 2004; Vol. C, p 922.

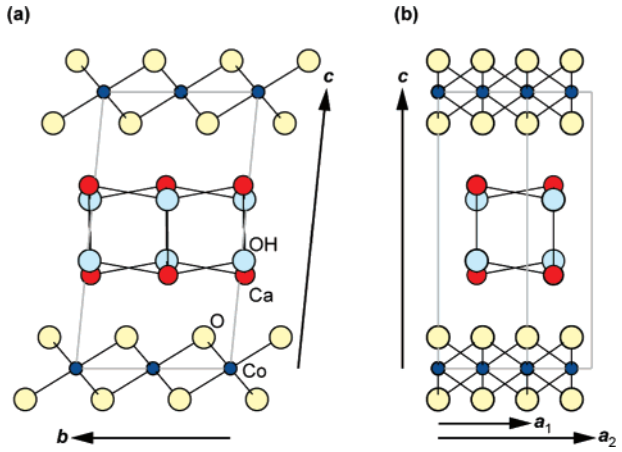

Figure 1. Fundamental structure of $(Ca_{0.85}OH)_{1.16}CoO_2$, projected along the [100] (a) and the [010] (b) directions. The gray-colored quadrilaterals represent unit cells of the subsystems.

Table 2. Refined Fractional Coordinates, $x^0_{\nu i}(j)$ ($\nu = 1, 2$, $i = 1, 2, 3$, $j =$ Co, O, Ca, OH), Occupation Factors, $p^0_\nu(j)$, and Isotropic Displacement Parameters, $B^0_\nu(j)$, for the Fundamental Structure of $(Ca_{0.85}OH)_{2\alpha}CoO_2$ ($\alpha = 0.57822$)

atom (j)	$x^0_{\nu 1}$	$x^0_{\nu 2}$	$x^0_{\nu 3}$	p^0_ν	B^0_ν (Å^2)
Subsystem 1 ($\nu = 1$): $[CoO_2]_\infty$					
Co	0	0	0	1.0[a]	0.5[a]
O	1/2	0.192(1)	0.1127(7)	1.0[a]	1.0[a]
Subsystem 2 ($\nu = 2$): $[2Ca_{0.85}OH]_\infty$					
Ca	1/4	0.0353(9)	0.6623(6)	0.85[a]	1.0[a]
OH	3/4	0.018(1)	0.610(1)	1.11111[a,b]	1.0[a]

[a] Fixed in the Rietveld refinement. [b] Correction in atomic scattering factors. (See text.)

same superspace-group symmetry as a monoclinic form of a layered sulfide, $(PbS)_{1.18}TiS_2$.[15] In this study we employed the centrosymmetric superspace group, $C2/m(\alpha 10)s0{-}C2_1/m(\alpha^{-1}\text{-}10)$, for the structure analysis of $(Ca_{0.85}OH)_{1.16}CoO_2$ and constructed an initial structure model, making reference to the structure model proposed by van Smaalen et al. for the monoclinic form of $(PbS)_{1.18}TiS_2$.[15] The fractional coordinates of the atoms in the fundamental structure of $(Ca_{0.85}OH)_{1.16}CoO_2$ were refined using the Rietveld analysis, in which no displacement modulation was taken into account. The resultant reliability factor, R_{wp}, was 0.1054. The parameters obtained are listed in Table 2. Fundamental structures a and b of Figure 1 are drawn using these parameters. The small value of R_{wp} is indicative of a reasonably good fit and consistency of the structure model.

For the refinement of the fundamental structure, atomic scattering factors of OH ions were replaced with those of the O ions. The occupation factor, p, of the site was set at 1.11111 to replicate the true atomic scattering factors of OH. This is because the atomic scattering factors of OH ions are estimated to be about $(Z+1)/Z$ times of the atomic scattering factors of O ions, where Z (=9) is the number of electrons of the O^- ions. Occupation factors, p, were set at 0.85 for the Ca site and at unity for all other sites. Isotropic atomic displacement parameters, B, were predefined at 0.5 Å^2 for the Co site and at 1.0 Å^2 for all other sites during the refinement. Coefficients for the analytical approximation of the atomic scattering factors for Co^{3+}, Ca^{2+}, and O^- were taken from Table 6.1.1.4 in ref 16. The preferred orientation due to a plate-like crystal habit was corrected using two preferred-orientation vectors of $\boldsymbol{c}^*$ (main direction) and $\boldsymbol{b}^*$ (subdirection). The 2θ range used in the analysis was from 11° to 70°, corresponding to the lattice-plane spacing, d, from 4.173 to 0.697 Å. The same conditions were also used for the following modulated-structure analysis.

Refinement of the Modulated Structure. For the (3 + 1)-dimensional composite crystal, the complete structure involves modulation for each atom. The atomic positions in the modulated structure can be described by the sum of the fundamental structure and deviations from them.[15,17−19] The coordinates of atom j of subsystem ν can be written as

$$x_{\nu i}(j) = \bar{x}_{\nu i}(j) + u^j_{\nu i}(\bar{x}_{\nu s4}) \quad (1)$$

($\nu = 1, 2$, $i = 1, 2, 3$, $j =$ Co, O, Ca, OH for the present case).

The first term in the right side is the fundamental structure. This term can be given by

$$\bar{x}_{\nu i}(j) = n_{\nu i} + x^0_{\nu i}(j) - (\mathbf{Z}^\nu_d t)_i \quad (2)$$

where $n_{\nu i}$ are integers describing the unit cell and $x^0_{\nu i}$ are the fractional coordinates of atom j within one unit cell of the fundamental structure. The fractional coordinates are given in Table 2. The matrix $\mathbf{Z}^\nu_d$ is defined by writing a $\mathbf{Z}$ matrix, $\mathbf{Z}^\nu$, as the juxtaposition of a 3×3 matrix $\mathbf{Z}^\nu_3$ and a $3 \times d$ matrix $\mathbf{Z}^\nu_d$ ($d = 1$): $\mathbf{Z}^\nu = (\mathbf{Z}^\nu_3 \mathbf{Z}^\nu_d)$. In the present case, the $\mathbf{Z}$ matrices for the subsystems are given by

$$\mathbf{Z}^1 = \begin{bmatrix} 1 & 0 & 0 & 0 \\ 0 & 1 & 0 & 0 \\ 0 & 0 & 1 & 0 \end{bmatrix}, \quad \mathbf{Z}^2 = \begin{bmatrix} 0 & 0 & 0 & 1 \\ 0 & 1 & 0 & 0 \\ 0 & 0 & 1 & 0 \end{bmatrix} \quad (3)$$

The t dependency of eq 2 reflects a shift of the origin with respect to that obtained with the standard superspace description for subsystem ν. This term is necessary to retain the relative phase between the subsystems when varying the physical space section $\mathbf{E}^3(t)$.

The second term of the right side of eq 1 represents the displacement modulation of the atoms. The modulation function of atom j can be written as a Fourier series:

$$u^j_{\nu i}(\bar{x}_{\nu s4}) = A^j_{0\nu i} + \sum_{n=1}^{m} [A^j_{ni} \cos(2\pi n \bar{x}_{\nu s4}) + B^j_{ni} \sin(2\pi n \bar{x}_{\nu s4})] \quad (4)$$

where $\bar{x}_{\nu s4}$ are the fourth superspace coordinates for the case, without modulation, in the subsystem superspace embedding.[15,17] The modulation function is periodic with periodicity 1 in its argument. The first term of the right side of eq 4 is for the correction of the basic structure in the refinement. The coordinates of the average structure are thus written as

$$\bar{x}'_{\nu i}(j) = \bar{x}_{\nu i}(j) + A^j_{0\nu i} \quad (5)$$

(15) van Smaalen, S.; Meetsma, A.; Wiegers, G. A.; de Boer, J. L. *Acta Crystallogr., Sect. B* **1991**, *47*, 314.
(16) Brown, P. J.; Fox, A. G.; Maslen, E. N.; O'Keefe, M. A.; Willis, B. T. M. In *International Tables for Crystallography*; Prince, E., Ed.; Kluwer: Dordrecht, 2004; Vol. C, p 578.
(17) van Smaalen, S.; de Boer, J. L. *Phys. Rev. B* **1992**, *46*, 2750.
(18) de Wolff, P. M. *Acta Crystallogr., Sect. A* **1974**, *30*, 777.
(19) Onoda, M. *J. Crystallogr. Soc. Jpn.* **1998**, *40*, 161; Onoda, M. *J. Crystallogr. Soc. Jpn.* **1998**, *40*, 202.

The fourth superspace coordinate $\bar{x}_{\nu s4}$ is given by

$$\bar{x}_{\nu s4} = \sigma_\nu \bar{x}_\nu + V_d^\nu t \tag{6}$$

where V_d^ν is the fourth element in the $\mathbf{V}^\nu$ matrix for the subsystem ν, and the σ-matrix represents the coordinates of the modulation wavevector $\boldsymbol{q}^\nu$.[15] For the present case, the $\mathbf{V}$ matrices and the σ-matrices of the subsystems are written as follows:

$$\mathbf{V}^1 = (0, 0, 0, 1), \quad \mathbf{V}^2 = (1, 0, 0, 0) \tag{7}$$

$$\sigma_1 = (\alpha, 0, 0), \quad \sigma_2 = (\alpha^{-1}, 0, 0) \tag{8}$$

The t-dependent part in eq 6 and the t dependence in $\bar{x}_{\nu i}(j)$, together define the relationship between the phases of the modulation functions in the two subsystems and the relative position of the subsystem lattices along the incommensurate direction.

For the four-dimensional system, the position of the atoms can be expressed using the coordinate vector (x_{s1}, x_{s2}, x_{s3}, x_{s4}) in four-dimensional real space. The relationship between x_{sk} (k = 1, 2, 3, 4) and $\bar{x}_{sk}$ is obtained as,

$$\begin{pmatrix} x_{s1} \\ x_{s2} \\ x_{s3} \\ x_{s4} \end{pmatrix} = \begin{pmatrix} \bar{x}_{s1} \\ \bar{x}_{s2} \\ \bar{x}_{s3} \\ \bar{x}_{s4} \end{pmatrix} + \mathbf{Y}^\nu \begin{pmatrix} u_{\nu 1}(\bar{x}_{\nu s4}) \\ u_{\nu 2}(\bar{x}_{\nu s4}) \\ u_{\nu 3}(\bar{x}_{\nu s4}) \end{pmatrix} \tag{9}$$

where $\mathbf{Y}^\nu$ is the pseudo-inverse of $\mathbf{Z}^\nu$. For the present case, $\mathbf{Y}^\nu$ is written by

$$\mathbf{Y}^1 = \begin{bmatrix} 1 & 0 & 0 \\ 0 & 1 & 0 \\ 0 & 0 & 1 \\ \alpha & 0 & 0 \end{bmatrix}, \quad \mathbf{Y}^2 = \begin{bmatrix} \alpha^{-1} & 0 & 0 \\ 0 & 1 & 0 \\ 0 & 0 & 1 \\ 1 & 0 & 0 \end{bmatrix} \tag{10}$$

The relationship between $\bar{x}_{sk}$ and the corresponding fundamental-structure position $\bar{x}_{\nu i}$ is expressed as,

$$\begin{pmatrix} \bar{x}_{s1} \\ \bar{x}_{s2} \\ \bar{x}_{s3} \\ \bar{x}_{s4} \end{pmatrix} = \mathbf{Y}^\nu \begin{pmatrix} \bar{x}_{\nu 1} \\ \bar{x}_{\nu 2} \\ \bar{x}_{\nu 3} \end{pmatrix} + \begin{pmatrix} 0 \\ 0 \\ 0 \\ t \end{pmatrix} \tag{11}$$

Figure 2 is an illustration of a unit cell in the four-dimensional real superspace and the relationship between the x_{sk} and $x_{\nu i}$ coordinates. Each cross section in superspace perpendicular to the additional dimension, $\mathbf{E}^3(t)$, gives an equivalent description of the physical space, $\mathbf{E}^3$. It is characterized using the parameter t, which is an element in another expression of the four-dimensional superspace coordinates (x, y, z, t). It should be noted that t can be defined as the distance from the three-dimensional real space and represents a position of a unit cell placed somewhere in the crystal.

The fourth coordinate of the subsystem superspace description, $\bar{x}_{\nu s4}$, is given in eq 6. Substitution of eqs 7 and 8 into eq 6 gives different expressions for the two subsystems:

$$\bar{x}_{1s4} = \alpha \bar{x}_{11}(j) + t = \alpha[n_{11} + x_{11}{}^0(j)] + t \tag{12a}$$

$$\bar{x}_{2s4} = \alpha^{-1} \bar{x}_{21}(j) = \alpha^{-1}[n_{21} + x_{21}{}^0(j) - t] \tag{12b}$$

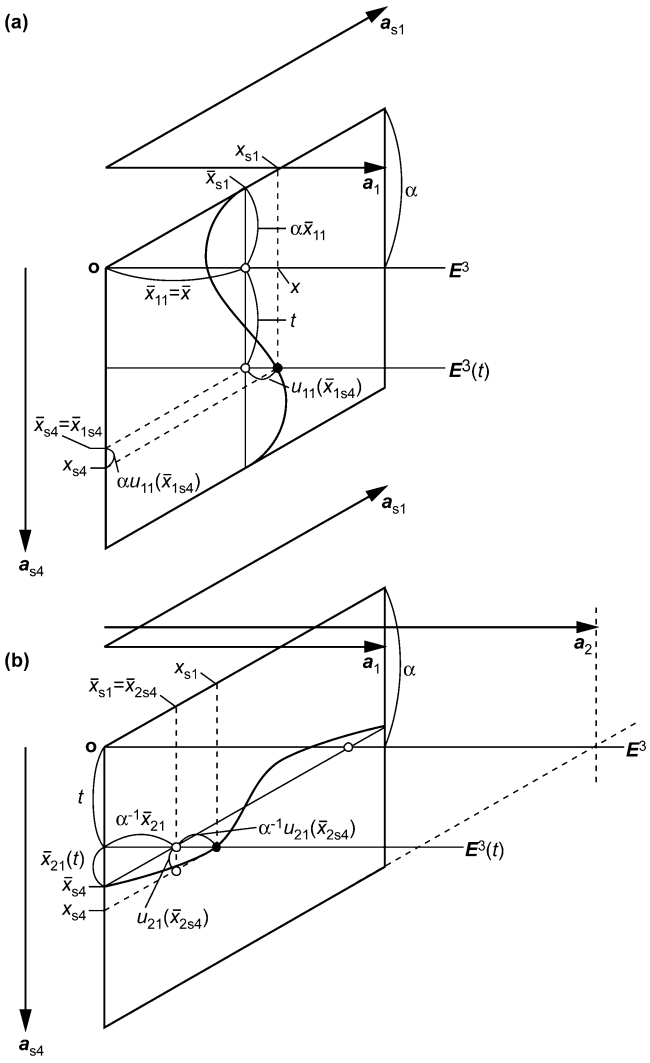

Figure 2. Description of a unit cell in the four-dimensional real superspace, and relationship between the coordinates, x_{sk} ($k = 1-4$) and $\bar{x}_{\nu i}$ (ν = 1, 2, i = 1, 2, 3): the structural modulations for the subsystem 1 (a) and for the subsystem 2 (b).

By substituting eqs 12a, 12b and 4 into eq 1, the coordinate $x_{\nu i}(j)$, and consequently the interatomic distances, can be expressed as a function of the fourth superspace coordinate t. By analogy, a similar expression for the modulation functions can be obtained for the modulation in the B and p parameters.[10,12]

The structure factor in a four-dimensional formalism is expressed as

$$F_{hklm} = \sum_j \int_0^1 d\bar{x}_{\nu s4} f(|\mathbf{h}|) \exp[2\pi i(hx_{s1} + kx_{s2} + lx_{s3} + mx_{s4})] \tag{13}$$

where $f(|\boldsymbol{h}|)$ are atomic scattering factors as a function of the three-dimensional reciprocal-lattice vector $\boldsymbol{h}$.[19] The structure analysis was carried out by comparing the calculated $|F_{hklm}|^2$ and the observed integral intensity of the reflections with $hklm$ indices. In the composite crystal each substructure is modulated because of the interaction between the substructures. The reciprocal base vectors of the first part ($\boldsymbol{a}_1$*, $\boldsymbol{b}$*, $\boldsymbol{c}$*) and those of the second part ($\boldsymbol{a}_2$*, $\boldsymbol{b}$*, $\boldsymbol{c}$*) are related to the minimal vector set in reciprocal space {$\boldsymbol{a}_1$*, $\boldsymbol{b}$*, $\boldsymbol{c}$*, $\boldsymbol{a}_2$*} through the $\mathbf{Z}$ matrices

Table 3. Restrictions Applying to Harmonic Amplitudes[a] in the Case of $C2/m(\alpha 10)s0-C2_1/m(\alpha^{-1}10)$

atom (*j*)		odd harmonics	even harmonics
	Subsystem 1 ($\nu = 1$): $[CoO_2]_\infty$		
Co	u_{11}	zero	odd
	u_{12}	odd	zero
	u_{13}	odd	zero
	p_1	zero	even
	B_1	zero	even
O	u_{11}	even	odd
	u_{12}	odd	even
	u_{13}	odd	even
	p_1	odd	even
	B_1	odd	even
	Subsystem 2 ($\nu = 2$): $[2Ca_{0.85}OH]_\infty$		
Ca	u_{21}	odd	odd
	u_{22}	even	even
	u_{23}	even	even
	p_2	even	even
	B_2	even	even
OH	u_{21}	odd	odd
	u_{22}	even	even
	u_{23}	even	even
	p_2	even	even
	B_2	even	even

[a] The "odd" means $A_n = 0$ and $B_n =$ variable; the "even" means $A_n =$ variable and $B_n = 0$; the "zero" means $A_n = B_n = 0$, where A_n ($n \geq 0$) and B_n ($n \geq 1$) are, respectively, the coefficients of cosine and sine components with the *n*-th harmonic order in the modulation function, eq 4.

in eq 3. The vectors in the minimal set are considered to be the projections of the base vectors of a four-dimensional reciprocal lattice. Thus, the two substructures are embedded in a four-dimensional structure and form two subsystems of the latter. In the computer program PREMOS the permutation matrix, $\mathbf{P}_\nu = (1,4)$ ($\nu = 2$: subsystem number), is used instead of the $\mathbf{Z}$ matrices.[20] The composite crystal is treated as an interpenetration of the two modulated structures. The subsystem superspace groups for the first and second subsystems listed in Table 1 are used in the present analysis. The modulation wave vectors selected for them are $\boldsymbol{a}_2^*$ and $\boldsymbol{a}_1^*$, respectively, based on the minimal vector set. Therefore, the reflections *hkl*0 and 0*klm* are main reflections for the first and the second parts. Furthermore, the reflection *hklm*, with both *h* and *m* nonzero, is the *m*th order satellite reflection of the first part and the *h*th order satellite reflection of the second part.

Parameter setting and refinement conditions for the present analysis are outlined as following. The maximum order of the harmonics, *m*, was set at 2 for the modulation functions in eq 4. Fourier amplitudes in $u^j_{\nu i}(\bar{x}_{\nu s4})$ were refined for all sites in the Rietveld analysis. Fourier amplitudes of *p* of the Ca atoms were also refined but the 0th order coefficient was set at zero to fix the average occupancy at $p^0{}_2$(Ca) (=0.85). *B* parameters were fixed at the initial values, B^0, for each site of the fundamental structure. For those sites that are special positions in the superspace group, all of the Fourier coefficients were not variable. Some of the Fourier coefficients in the modulation functions should be fixed at null because of the constraints. Restrictions applying to harmonic amplitudes in case of $C2/m(\alpha 10)s0-C2_1/m(\alpha^{-1}10)$ are summarized in Table 3. As a result, the modulation functions of u_{11}, u_{12}, and u_{13} for Co, and u_{21} for Ca and OH are odd functions, while the modulation functions of *p* and *B* for Co, and u_{22}, u_{23}, *p*, and *B* for Ca and OH are even functions. The total number of parameters refined in the analysis was 61, including 29 Fourier amplitudes in the modulation functions for the fractional coordinates and the occupation factor.

(20) Yamamoto, A. *Acta Crystallogr., Sect. A* **1992**, *48*, 476.

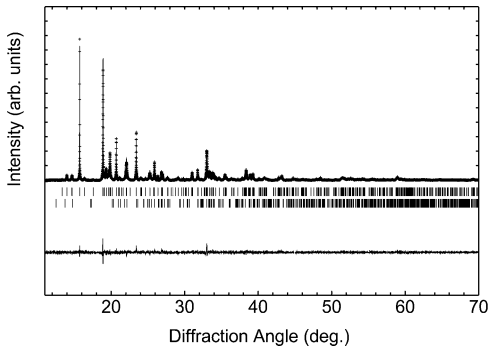

Figure 3. Rietveld-refinement pattern of the synchrotron X-ray diffraction data for $(Ca_{0.85}OH)_{2\alpha}CoO_2$ ($\alpha = 0.57822$). The upper solid line is calculated intensities. The small crosses superimposed on it are observed intensities. The lower solid line is differences between the observed and calculated intensities. Short vertical lines below the profiles indicate the peak positions of the main (upper) and satellite (lower) reflections for the two subsystems.

Table 4. Crystallographic Data and Structure Refinement for $(Ca_{0.85}OH)_{2\alpha}CoO_2$ ($\alpha = 0.57822(8)$)

formula	$(Ca_{0.85}OH)_{2\alpha}CoO_2$ ($\alpha = 0.57822(8)$)
fw	149.996
temp	295 K
synchrotron X-ray wavelength	0.8 Å (15497.68 eV)
diffractometer	BL15XU at SPring-8, JASRI
crystal system	monoclinic (subsystem-1) monoclinic (subsystem-2)
superspace group	$C2/m(\alpha 10)s0-C2_1/m(\alpha^{-1}10)$
lattice constants	$a_1 = 2.8180(4)$ Å $b = 4.8938(6)$ Å $c = 8.810(1)$ Å $\cos\alpha_0 = -0.10022(5)$, viz., $\alpha_0 = 95.75(3)°$ $\alpha(=a_1/a_2) = 0.57822(8)$, viz., $a_2 = 4.8736(4)$ Å
cell volume	120.88(2) Å^3 (subsystem-1)
Z	2
density(calcd)	4.121 g/cm^3
2θ range used	11−70° in 0.005° steps
no. of observations used	11650
no. of reflections	915 main: 353 (70 (0*kl*0), 152 (*hkl*0), 131 (0*klm*)), satellite: 562 (*hklm*)
no. of refined parameters	Fourier amplitudes: 29, others: 32
R-factors	$R_{wp} = 8.51\%$, $R_p = 6.46\%$, $R_e = 15.8\%$, $S(=R_{wp}/R_e) = 0.537$ $R_I = 3.97\%$, $R_F(=R) = 1.76\%$, $R_w = 2.51\%$
refinement software	PREMOS2k*i*, PREMOS91

Results

Figure 3 is the best Rietveld-refinement result in the case of the modulated structure. This figure indicates the observed, calculated, and difference patterns for the synchrotron X-ray powder diffraction data. The Rietveld-refinement details and characteristics of the final refinement are summarized in Table 4. The resultant profile reliability factor, $R_{wp} = 0.0851$, is already at the practical minimum limit. There has been much tweaking of the trials to try to improve the Rietveld-analysis convergence. The still somewhat high R_{wp} implies imperfect profile fitting. This is presumably due to a somewhat insufficient approximation to the precise shape of the modulation functions, or the

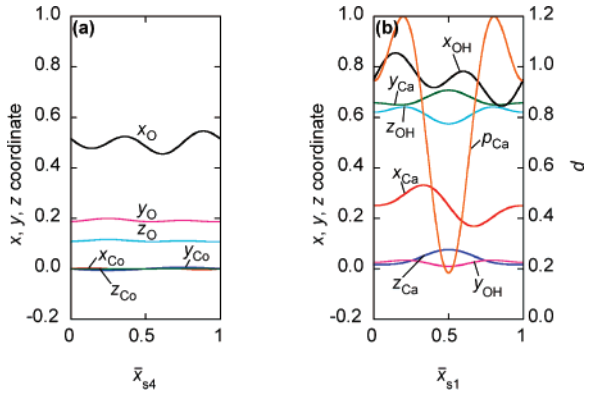

Figure 4. Modulation of the fractional coordinates, x, y, z ($=x^0_{\nu i}+u_{\nu i}$: $\nu = 1, 2$, $i = 1, 2, 3$), and the occupation factor, p, for the atoms in $(Ca_{0.85}OH)_{2\alpha}CoO_2$ ($\alpha = 0.57822$): (a) subsystem 1 and (b) subsystem 2. The parameters are plotted as a function of the fourth superspace coordinate, $\bar{x}_{s4}(=\bar{x}_{1s4})$ for Co and O, and $\bar{x}_{s1}(=\bar{x}_{2s4})$ for Ca and OH.

Table 5. Fourier Amplitudes Obtained from the Rietveld Refinement of $(Ca_{0.85}OH)_{2\alpha}CoO_2$ ($\alpha = 0.57822$). A_n ($n = 0-2$) and B_n ($n = 1, 2$) Are, Respectively, the Coefficients of Cosine and Sine Components with the nth Harmonic Order in the Modulation Function, Eq 4[a]

atom (j)		A_0	A_1	B_1	A_2	B_2
		Subsystem 1 ($\nu = 1$): $[CoO_2]_\infty$				
Co	u_{11}					0.003(2)
	u_{12}			−0.006(1)		
	u_{13}			−0.000(1)		
O	u_{11}		0.015(7)			−0.034(5)
	u_{12}	−0.001(1)		0.004(4)	−0.004(5)	
	u_{13}	−0.0017(6)		0.002(2)	−0.002(3)	
		Subsystem 2 ($\nu = 2$): $[2Ca_{0.85}OH]_\infty$				
Ca	u_{21}			0.063(6)		−0.030(9)
	u_{22}	0.004(1)	−0.030(3)		0.007(5)	
	u_{23}	0.006(2)	−0.024(2)		0.013(3)	
	p_2	0.0[b]	0.38(5)		−0.2(1)	
OH	u_{21}			0.052(5)		0.066(7)
	u_{22}	0.007(2)	0.007(6)		−0.00(1)	
	u_{23}	0.006(1)	0.023(5)		−0.020(7)	

[a] Numbers in parentheses are estimated standard deviations of the last significant digit. Blank columns represent a null coefficient, derived from the constraint on the special position of the site. (See Table 3.) [b] Fixed in the Rietveld refinement to fix the average occupancy at p^0_2(Ca) (=0.85).

peculiar broad profile shape of the Bragg reflections in the layered crystal. Nevertheless, the small R_F (=0.0176) ensures that the structure model and the refined parameters are reliable.

Table 5 lists refined Fourier amplitudes of the modulation functions. A_n ($n = 0-2$: order of the harmonics) and B_n ($n = 1, 2$) are, respectively, the coefficients of the cosine and sine components in the modulation function, eq 4; numbers in parentheses are estimated standard deviations of the last significant digit. Blank columns represent a null coefficient, derived from the constraint on the crystallographically special position of the site. The modulation of the fractional coordinates, $u_{\nu i}$, and the occupation factors, p_ν, of the atoms can be calculated with eqs 1, 2, and 4 using the obtained parameters in Table 2 and 5. The $u_{\nu i}$ and p_ν parameters are plotted in Figure 4 as a function of the fourth superspace coordinate, $\bar{x}_{\nu s4}$ ($=\bar{x}_{s4}$ for Co and O, or $=\bar{x}_{s1}$ for Ca and OH). Figure 5 represents the four-dimensional description of the positional parameters of the atoms, plotted as wavy strings on the $\boldsymbol{a}_{s1}-\boldsymbol{a}_{s4}$ cross section in the four-dimensional real superspace.

Average-structure parameters for the modulated crystal can be obtained by adding A_0 in Table 5 to the corresponding

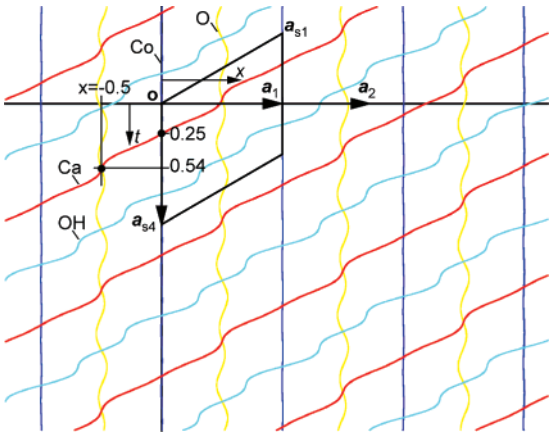

Figure 5. Four-dimensional description of the incommensurate composite crystal $(Ca_{0.85}OH)_{2\alpha}CoO_2$ ($\alpha = 0.57822$). The horizontal line represents the physical coordinate along the $\boldsymbol{a}_1$ and $\boldsymbol{a}_2$ axis, and t is the complementary coordinate. Atoms are depicted as wavy strings; the lines represent Co (blue), O (yellow), Ca (red), and OH (light-blue). The $\boldsymbol{a}_{s1}$ and $\boldsymbol{a}_{s4}$ represent the periodicity in four-dimensional superspace. The solid parallelogram corresponds to a unit cell drawn in Figure 2. Average coordinates of the atoms marked are Co (0, 0, 0), O (0.5, 0.191, 0.1110), Ca (0.25, 0.039, 0.668), and OH (0.75, 0.025, 0.617).

Table 6. Fractional Coordinates of the Average Structure of $(Ca_{0.85}OH)_{2\alpha}CoO_2$: $x^0_{\nu i}(j) + A_{0\nu i}$ ($\nu = 1, 2$, $i = 1, 2, 3$, $j =$ Co, O, Ca, OH)

atom (j)	$x^0_{\nu 1}+A_{0\nu 1}$	$x^0_{\nu 2}+A_{0\nu 2}$	$x^0_{\nu 3}+A_{0\nu 3}$
	Subsystem 1 (ν=1): $[CoO_2]_\infty$		
Co	0	0	0
O	1/2	0.191(1)	0.1110(6)
	Subsystem 2 (ν=2): $[2Ca_{0.85}OH]_\infty$		
Ca	1/4	0.039(1)	0.668(2)
OH	3/4	0.025(2)	0.617(1)

fundamental-structure parameters in Table 2. The average-structure coordinates are listed in Table 6. Selected interatomic distances and bond angles of the average structure are listed in Table 7. Figure 6 is a schematic drawing of a part of the crystal structure, highlighting the atomic coordination around the Co and Ca atoms.

All the interatomic distances, l, included in the modulated crystal can be plotted as a function of a complementary coordinate, i.e., the fourth superspace coordinate, t. Figures 7, 8, 9 and 10 are plots of t versus distance, l(Co−O), l(Ca−OH), l(Ca−O), and l(OH−O), respectively. Note that l is periodic in the interval $0 \le t \le 1.0$ for the Co−O distances and in the interval $0 \le t \le a_1/a_2(=\alpha=0.57822(8))$ for the Ca−OH, Ca−O, and OH−O distances. The Co−O and Ca−OH distances are intrasubsystem, while the Ca−O and OH−O distances are intersubsystem. The variation of the intrasubsystem distances implies that displacement modulations are more pronounced in the $[2Ca_{0.85}OH]$ subsystem than in $[CoO_2]$. In Figures 7, 8, 9, and 10, the numbers listed beside the interatomic distance waves correspond to the numbers assigned to the O or OH atoms in Figure 6. The modulation amplitudes of the selected interatomic distance waves are summarized in Table 6.

Discussion

Overall Features of the Structure. The fundamental crystal structure of $(Ca_{0.85}OH)_{1.16}CoO_2$ is illustrated in Figure 1. Basically, the structure is built up with CoO_2 layers (subsystem-1) and rock-salt-type double $Ca_{0.85}OH$ layers (subsystem-2)

Table 7. Selected Interatomic Distances and Bond Angles for the Average and Modulated Structures of $(Ca_{0.85}OH)_{2\alpha}CoO_2$ ($\alpha = 0.57822$)

	length (Å) or angle (deg)	
bond/angle	average structure	modulated structure (shortest–longest)
	Intrasubsystem ($\nu = 1$)	
$Co-O^{1,2,4,5}$	1.91	1.82−1.98
$Co-O^{3,6}$	1.88	1.86−1.90
$Co-O^{1,5}-Co^{1}$	95	93−96
	Intrasubsystem ($\nu = 2$)	
$Ca-OH^{1,2}$	2.48	1.94−3.05
$Ca-OH^{3}$	2.47	2.40−2.60
$Ca-OH^{4}$	2.51	2.41−2.74
$Ca-OH^{5}$	2.51	2.44−2.58
$Ca-OH^{1}-Ca^{1}$	159	142−170
$Ca-OH^{3}-Ca^{2}$	159	136−166
$Ca-OH^{1}-Ca^{3}$	88	69−112
$Ca-OH^{3}-Ca^{3}$	89	69−107
$Ca-OH^{1,5}-Ca^{4}$	101	85−124
	(shortest–longest)	
	Intersubsystem	
Ca−O*(the first nearest neighbor)	2.23−2.40	2.17−2.54
Ca−O* (the second nearest neighbor)	2.40−2.73	2.29−2.75
Ca−O* (the third nearest neighbor)	2.64−3.60	2.32−3.18
OH^{1}−O* (the first nearest neighbor)	2.64−2.77	2.58−3.01
$Co-O^{4,5}-Ca$ ($0.140 \le t \le 0.355$)	70−84	73−88
$Co-O^{6}-Ca$ ($0.140 \le t \le 0.355$)	91−91	91−91

[a] The fundamental-structure positions of the atoms at $t = 0$ are: Co = (x^0_{11}, x^0_{12}, x^0_{13}+1), Co^1 = (x^0_{11}+1, x^0_{12}, x^0_{13}+1), O^1 = (x^0_{11}, x^0_{12}, x^0_{13}+1), O^2 = (x^0_{11}−1, x^0_{12}, x^0_{13}+1), O^3 = (x^0_{11}−1/2, x^0_{12}−1/2, x^0_{13}+1), O^4 = (−x^0_{11}, −x^0_{12}, −x^0_{13}+1), O^5 = (−x^0_{11}+1, −x^0_{12}, −x^0_{13}+1), O^6 = (−x^0_{11}+1/2, −x^0_{12}+1/2, −x^0_{13}+1), O* = (−x^0_{11}+n_{11}, −x^0_{12}, −x^0_{13}+1) or (−x^0_{11}+n_{11}+1/2, −x^0_{12}+1/2, −x^0_{13}+1), Ca = (x^0_{21}, x^0_{22}, x^0_{23}), Ca^1 = (x^0_{21}+1, x^0_{22}, x^0_{23}), Ca^2 = (x^0_{21}, x^0_{22}+1, x^0_{23}), Ca^3 = (x^0_{21}+1, x^0_{22}+1, x^0_{23}), Ca^4 = (−x^0_{21}+1, −x^0_{22}, −x^0_{23}+1), OH^1 = (x^0_{21}, x^0_{22}, x^0_{23}), OH^2 = (x^0_{21}−1, x^0_{22}, x^0_{23}), OH^3 = (x^0_{21}−1/2, x^0_{22}+1/2, x^0_{23}), OH^4 = (x^0_{21}−1/2, x^0_{22}−1/2, x^0_{23}), OH^5 = (−x^0_{21}+1, x^0_{22}, −x^0_{23}+1), where x^0_{vi} (ν = 1, 2 and i = 1, 2, 3) are the fractional coordinates of the atoms listed in Table 2. The superscript numbers of the anions refer to the atom numbers assigned in Figure 6.

alternately stacked along the *c*-axis. The CoO_2 layer is composed of edge-sharing CoO_6 octahedra. The Co and O atoms form a triangle lattice for each atomic plane. The $Ca_{0.85}OH$ block is not of the ideal rock-salt-type structure but is initially deformed because of the large difference in the *z*-coordinate position of the Ca and OH ions. This is because the Coulombic force between the O^{2-} ions and the Ca^{2+} ions is attractive and is repulsive between the O^{2-} ions and the OH^- ions.

Figure 11 represents projection views along the *a*-, *b*-, and *c*-axes of the modulated crystal structure, illustrated using the refined structure parameters. Undulated rows of the O atoms can be observed in the $[CoO_2]$ subsystem. Displacement of the Co atoms is small. In contrast, large displacement modulation was observed in the $[2Ca_{0.85}OH]$ subsystem. The amplitude of the modulation is attributed to the strength of the intersubsystem interaction. Since the O and $Ca_{0.85}OH$ planes are situated close to the misfit-layer boundary between the two subsystems, the incommensurability between the subsystems should more directly deform the structures. In contrast, the Co atoms are situated so as to withdraw into the close-packed CoO_6 octahedron shells, which could possibly screen out or moderate the incommensurable intersubsystem Coulombic interaction. The structural modulation in the $Ca_{0.85}OH$ atomic planes and the CoO_2 layer are illustrated in Figure 11c. From the cross sections (i−iii), a large in-plane deformation can be observed in each $Ca_{0.85}OH$ plane. A similar local deformation repeatedly appears every four times of a_2 for the subsystem 2 and every seven times of a_1 for the subsystem 1, because the incommensurable ratio of the lattices, a_1/a_2 (=0.57822), is nearly equal to 4/7 (=0.57143).

Structure in the CoO_2 subsystem. The Co ion coordinates with six neighboring O ions. As illustrated in Figure 11, the displacement of the atoms in the CoO_2 layers is not that much larger than that in the $Ca_{0.85}OH$ layers. The displacement is particularly small for the Co atoms. The modulation in the CoO_2 layer is due mainly to the O atoms. With constraints on inversion symmetry in the adopted superspace group, $C2/m(\alpha 10)s0-C2_1/m(\alpha^{-1}10)$, the Co−O bond lengths are basically restricted to two types. In Figure 7, the modulated waves of the bonds, numbers 1, 2, 4, and 5, which have different phases of the wave function, are essentially the same. The modulated waves of the bonds, numbers 3 and 6, are also the same. The bonds, numbers 1, 2, 4, and 5, modulate in the range of $1.82 \le l \le 1.98$ Å, while the other type of bonds, numbers 3 and 6, modulate in the range of $1.86 \le l \le 1.90$ Å. In both cases, the amplitudes of the undulation of the Co−O bond lengths are comparatively small. The average Co−O bond lengths are 1.91 Å for the bonds 1, 2, 4, and 5, and 1.88 Å for the bonds 3 and 6. These values are slightly shorter than the value 1.945 Å, which is estimated from the summation of the effective ionic radii of Co and O −0.545 Å for Co^{3+} (six-fold coordination with a low-spin state) and 1.40 Å for O^{2-} (six-fold coordination).[21] The shortened Co−O bond lengths indicate that the Co ions attract the surrounding O ions, due to the higher cobalt valence; viz., holes are introduced into the Co t_{2g} band. Actually, the cobalt valence of the present compound, $(Ca_{0.85}OH)_{1.16}CoO_2$ was reported to be +3.16.[7] The observed shorter Co−O bond length is consistent with this result.

For a series of layered cobalt oxides, CoO_6 octahedra are deformed when compared with a cubic symmetrical octahedron. In particular, in hole-doped compounds the Co−O ion interaction is an attractive Coulombic force, which flattens out the

(21) Shannon, R. D. *Acta Crystallogr., Sect. A* **1976**, *32*, 751.

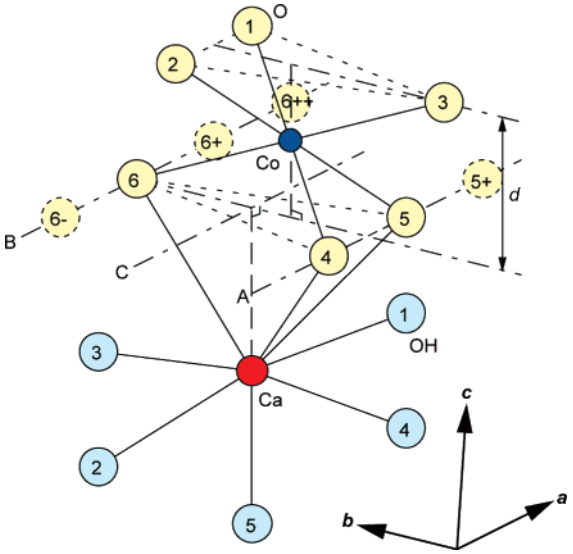

Figure 6. Schematic drawing of a part of the crystal structure, highlighting the atomic coordination around the Co and Ca atoms at $t \approx 0.25$. The numbers on the atoms refer to the curve numbers in Figures 7, 8, 9, and 10. d is the thickness of the CoO_2 layer.

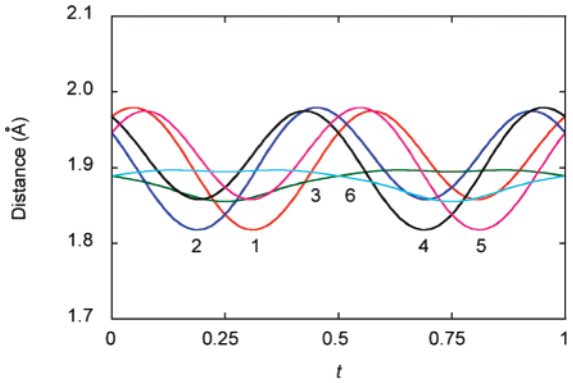

Figure 7. Intrasubsystem interatomic distances between Co ($\nu = 1$) and O ($\nu = 1$) in the modulated structure of $(Ca_{0.85}OH)_{2\alpha}CoO_2$ ($\alpha = 0.57822$). The curve numbers refer to the O ion numbers in Figure 6.

CoO_6 octahedra along the c-axis. The thickness of the CoO_6 octahedron, d, is therefore often used as a measure of the hole-doping level. In the present case of $(Ca_{0.85}OH)_{1.16}CoO_2$, the thickness d modulates in the range of $1.91 \leq d \leq 2.04$ Å, about 1.96 Å on average. The average d value, 1.96 Å, is shorter than that measured for non-doped orthorhombic $(CaOH)_{1.14}CoO_2$ ($Co^{2.94+}$, $d \approx 2.05$ Å),[5,6] but is longer than the superconducting sodium cobalt oxides, such as $Na_{0.343}(H_3O)_{0.237}CoO_2 \cdot 1.19H_2O$ (BLH-Na_xCoO_2 ($P2$): $Co^{3.43+}$, $d \approx 1.80$ Å)[22] or $Na_{0.35}(H_3O)_{0.17}(H_2O)_{1.22}CoO_2$ (BLH-Na_xCoO_2 ($P3$): $Co^{3.48+}$, $d \approx 1.85$ Å).[23] The d value of $(Ca_{0.85}OH)_{1.16}CoO_2$ is, if anything, near to the value of the moderately hole-doped prototype compound, γ-$Na_{0.711}CoO_2$ ($Co^{3.289+}$, $d \approx 1.96$ Å).[24]

It is well-known that the bond-valence sum (S_{ij}) is an empirical measure of oxidation states for cations in inorganic solids.[25,26] Figure 12 is a plot of S_{ij} as a function of the fourth superspace coordinate, t, for the Co atoms in $(Ca_{0.85}OH)_{1.16}CoO_2$.

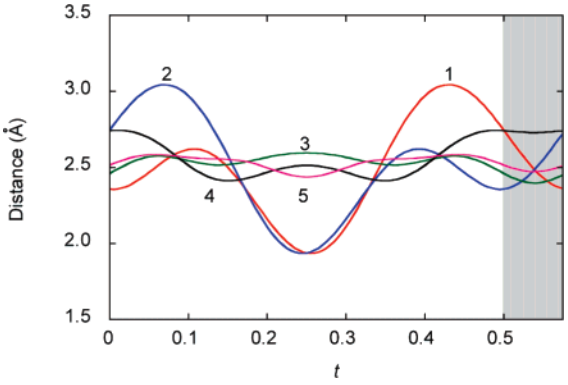

Figure 8. Intrasubsystem interatomic distances between Ca ($\nu = 2$) and OH ($\nu = 2$) in the modulated structure of $(Ca_{0.85}OH)_{2\alpha}CoO_2$ ($\alpha = 0.57822$). The curve numbers refer to the OH ion numbers in Figure 6. The hatched area is related to the Ca defect, and thus the Ca−OH bond lengths in this area actually do not exist in the structure.

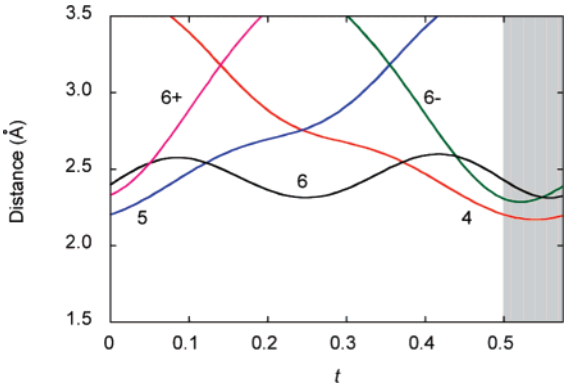

Figure 9. Modulated-structure interatomic distances between Ca ($\nu = 2$) and O ($\nu = 1$) as a function of the fourth superspace coordinate t. The curve numbers refer to the O ion numbers in Figure 6. The hatched area is related to the Ca defect, and thus the Ca−O bond lengths in this area actually do not exist in the structure.

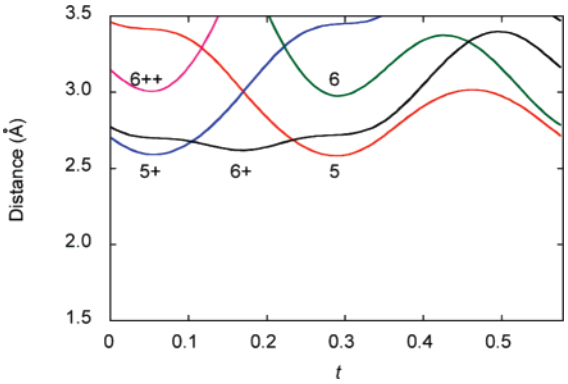

Figure 10. Modulated-structure interatomic distances between OH ($\nu = 2$) and O ($\nu = 1$) as a function of the fourth superspace coordinate t. The curve numbers refers to the O ion numbers in Figure 6.

The S_{ij} values were calculated using the Co−O distances in Figure 7. The S_{ij} values are proportional to a probability of hole occupancy at each Co site, and the amplitude of the S_{ij} modulation wave can be regarded as a scale of the potential modulation in the CoO_2 conduction layer. The S_{ij} modulates in the range of +3.1 to +3.8, and is +3.4 on average. However, the S_{ij} values seem to be overestimated compared to the true Co valence, +3.16, determined from a chemical analysis.[7] In

(22) Takada, K.; Fukuda, K.; Osada, M.; Nakai, I.; Izumi, F.; Dilanian, R. A.; Kato, K.; Takata, M.; Sakurai, H.; Takayama-Muromachi, E.; Sasaki, T. *J. Mater. Chem.* **2004**, *14*, 1448.
(23) Takada, K.; Sakurai, H.; Takayama-Muromachi, E.; Izumi, F.; Dilanian,R. A.; Sasaki, T. *Adv. Mater.* **2004**, *16*, 1901.
(24) Huang, Q.; Khaykovich, B.; Chou, F. C.; Cho, J. H.; Lynn, J. W.; Lee, Y. S. *Phys. Rev. B* **2004**, *70*, 134115.
(25) Brown, I. D.; Altermatt, D. *Acta Crystallogr., Sect. B* **1985**, *41*, 244.
(26) Brese, N. E.; O'Keeffe, M. *Acta Crystallogr., Sect. B* **1991**, *47*, 192.

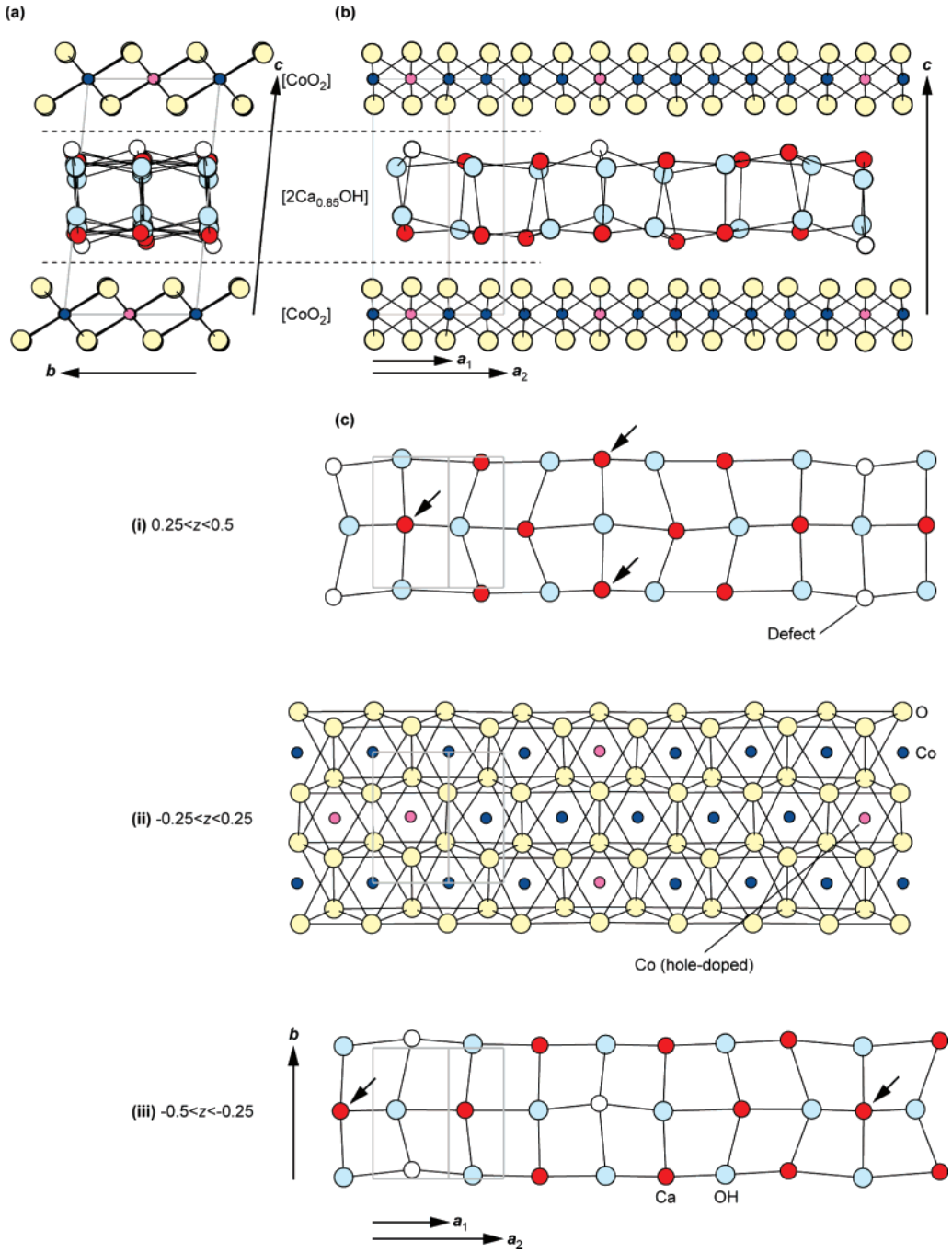

Figure 11. Modulated structure of $(Ca_{0.85}OH)_{2\alpha}CoO_2$ ($\alpha = 0.57822$) projected along the [100] (a), the [010] (b), and the [00−1] (c) directions. In (a) and (b) the drawn space is within $0 \le x \le 7$, $0 \le y \le 1$, and $0 \le z \le 1$ for the Co atoms and its vicinity. The broken lines represent misfit-layer boundaries between the $[CoO_2]$ and $[2Ca_{0.85}OH]$ subsystems. Figure (c) shows cross sections at (i) $0.25 < z < 0.5$ (the upper $Ca_{0.85}OH$ plane), (ii) $-0.25 < z < 0.25$ (the CoO_2 layer), and (iii) $-0.5 < z < -0.25$ (the lower $Ca_{0.85}OH$ plane). The gray-colored quadrilaterals represent unit cells of the subsystems. The small pink circles in the Co layer represent possible hole-doped Co sites. The white circles in the $Ca_{0.85}OH$ layers represent possible defect sites. The arrows represent "the most deformed part". (See text.)

the case of modulated crystals, the "absolute" value of S_{ij} may be less reliable for the determination of the accurate valence, since the bond-valence sum method is merely an empirical rule established for standard inorganic solids. The use of the bond-valence sum method, for modulated crystals, should therefore be limited to the cases where a relative evaluation is performed.

$[Ca_2(Co_{0.65}Cu_{0.35})_2O_4]_{0.63}CoO_2$ is a hole-doped misfit-layer compound with quadruple atomic layers in the rock-salt-type block. Structure parameters of this phase were reported previously.[27] The S_{ij} values are also shown in Figure 12 for comparison. Both the S_{ij} waves for $(Ca_{0.85}OH)_{1.16}CoO_2$ and $[Ca_2(Co_{0.65}Cu_{0.35})_2O_4]_{0.63}CoO_2$ are quite similar in terms of the average value and the amplitudes of the modulation. It suggests that the hole-doping level and the degree of the potential modulation in the CoO_2 conduction layer for $(Ca_{0.85}OH)_{1.16}CoO_2$ are not significantly different from those of $[Ca_2(Co_{0.65}Cu_{0.35})_2O_4]_{0.63}CoO_2$.

The structural modulation in the CoO_2 layer should induce different electrostatic potential at the Co sites through the difference of the surrounding Co−O bond-lengths. It can be

(27) Miyazaki, Y.; Miura, T.; Onoda, M.; Uchida, M.; Ishii, Y.; Ono, Y.; Morii, Y.; Kajitani, T. *Jpn. J. Appl. Phys.* **2003**, *42*, 7467.

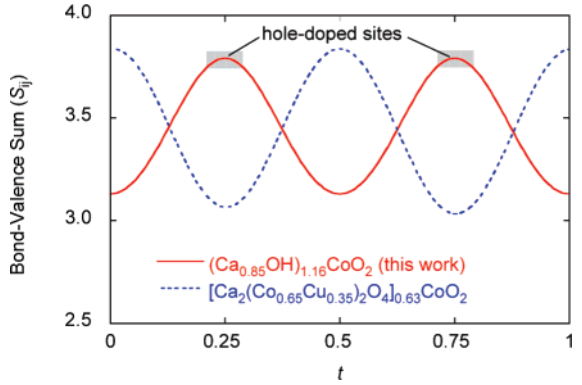

Figure 12. Bond-valence sum (S_{ij}) values of the Co atoms in $(Ca_{0.85}OH)_{2\alpha}$-CoO_2 ($\alpha = 0.57822$), plotted as a function of the fourth superspace coordinate t (solid line). The S_{ij} values were calculated using the Co−O distances in Figure 7. Holes are expected to be introduced at the $t \approx 0.25$ and $t \approx 0.75$ sites. (See text.) S_{ij} values for $[Ca_2(Co_{0.65}Cu_{0.35})_2O_4]_{0.63}CoO_2$[25] are also drawn in the figure for comparison (broken line).

expected that holes tend to be localized at lower electrostatic potential sites. The bond-valence sum is a good scale of the electrostatic potential and is useful for estimating the probable sites where holes are localized at the ground state. In Figure 12 the S_{ij} of $(Ca_{0.85}OH)_{1.16}CoO_2$ exhibit maxima at $t = 0.25$ and $t = 0.75$. This suggests that holes are expected to be located at the Co sites where $t \approx 0.25$ and $t \approx 0.75$. As illustrated in Figure 6 and 7, three upper O atoms, number 1, number 2, and number 3, approach the Co atom at $t \approx 0.25$, while another set of three O atoms, numbers 4, 5, and 6, approach the Co atom at $t \approx 0.75$. Assuming that the holes are situated only at the sites within the ranges of $t = 0.25 \pm 0.04$ and $t = 0.75 \pm 0.04$, we can determine the arrangement of the hole-doped sites in real space, where the width of the range of t, 0.04, was estimated from the hole concentration, 0.16.[7] In Figure 11, the possible arrangement of the hole-doped Co sites is illustrated with small pink circles.

Structure in the CaOH Subsystem. The most remarkable structural feature in $(Ca_{0.85}OH)_{1.16}CoO_2$ is the large deformation of the atomic arrangement in the $[2Ca_{0.85}OH]$ subsystem. The $Ca_{0.85}OH$ block is markedly distorted and is different from an ideal rock-salt-type structure. The similar tendency is observed for orthorhombic $(CaOH)_{1.14}CoO_2$.[6] The Ca atom coordinates with five OH ions in the $[2Ca_{0.85}OH]$ subsystem and with three O ions in the $[CoO_2]$ subsystem (See Figure 6). Among the five Ca−OH bonds, one bond is made up of an OH ion in the neighboring plane (bond 5), while the remaining four bonds are made up of OH ions in the same plane to which the Ca atom belongs (bonds 1−4). The Ca−OH bond lengths of an average structure are 2.48, 2.48, 2.47, 2.51, and 2.51 Å for the bonds 1, 2, 3, 4, and 5, respectively. All the average values are nearly equal to the value 2.49 Å, which is estimated from the summation of the effective ionic radii of Ca and OH − 1.12 Å for Ca^{2+} (eight-fold coordination) and 1.37 Å for OH^- (six-fold coordination).[21]

As shown in Figure 8 and Table 7, the Ca−OH bond lengths modulate in the range of $1.94 \leq l \leq 3.05$ Å for the bonds 1 and 2, $2.40 \leq l \leq 2.60$ Å for bond 3, $2.41 \leq l \leq 2.74$ Å for bond 4, and $2.44 \leq l \leq 2.58$ Å for bond 5. The amplitudes of the bond-length waves, 3, 4, and 5, are ordinary. However, the markedly large modulation was observed for bonds 1 and 2. Both bonds 1 and 2 simultaneously take the considerably short length at $t \approx 0.25$. The short length is principally due to large amplitude of the modulation function of the x component of the OH ions (See Figure 4b). When $t = 0.25$ for the Ca atom, the two neighboring OH ions in front and behind of the Ca atom take the minimum and maximum x-coordinates, respectively. The OH ions simultaneously approach the Ca atom along the a-axis. In Figure 11c, the corresponding Ca sites are marked with arrows, where the symmetrical large intraplane deformation appears. Numbers 3 and 4 OH ions, i.e., two OH ions adjoining the marked Ca sites along the b-axis direction, look to be either driven downward or upward in order to maintain their distance from the number 1 and number 2 OH ions. In this paper, we hereafter call this local part "the most deformed part".

Fifteen percent of the Ca sites are defective. It was found in Figure 4b that the modulation function of occupancy, p, of the Ca atom exhibits a significant modulation, which abruptly approaches zero at $x_{s1} = 0.5$.[28] This suggests that the Ca defects are expected to be concentrated around the $x_{s1} = 0.5$ position in superspace coordinates. For simplification, in this paper, we assume that the Ca-defect sites are situated selectively at the sites within the range of $x_{s1} = 0.5 \pm 0.075$, where the width of the range of x_{s1} was estimated from the amount of the Ca defects, 0.15. In Figure 8 the Ca-defect sites are in the region where $t > 0.5$ (the "hatched" area), in which the Ca−OH bond lengths in the range $t = 0.54 \pm 0.04$ do not exist. In the hatched area, the tentative five Ca−OH bond lengths look to be relatively balanced compared to those outside of the hatched area. This implies that the Ca defect may occur at local sites in which the structural deformation is not large ("the small modulation part"). In Figure 11 possible Ca-defect sites are illustrated with white circles.

In ionic crystals, the defect of ions is dependent on the electrostatic potential at the site. At the "most deformed part", the minimum Ca−OH bonds produce a low electrostatic potential at the Ca site. At the low potential site, the Ca ion can be situated more stably. This explains the total (100%) occupancy of Ca at the "most deformed part". In contrast, the "small modulation part" has higher electrostatic potential than the "most deformed part". At the high potential site, the Ca ion is too unstable to be situated. This explains the analysis result that the Ca atoms tend to be deficient at the "small modulation part".

Structural Relation between the Subsystems. As seen in Figure 6, the Ca atoms (and also OH ions) are situated below (or above) the center line, (line C) equidistant from the two neighboring O rows (lines A and B) running along the a-axis, to equilibrate the Coulombic force. The Ca atom coordinates with three O atoms in the adjoining CoO_2 layer. As in Figure 9 and Table 7, the Ca−O interatomic distance modulates. The local structure, i.e., relative position between the Ca atom and the three O atoms, varies from site to site because of the incommensurability between the subsystem lattices. The modulation ranges of the Ca−O interatomic distance are $2.17 \leq l \leq 2.54$ Å for the first nearest neighbor (first NN) atom, $2.29 \leq l \leq 2.75$ Å for the second nearest neighbor (second NN) atom, and $2.32 \leq l \leq 3.18$ Å for the third nearest neighbor (third NN) atom. The average distances are 2.36, 2.54, and 2.75 Å

(28) Strictly speaking, the modulation function of p is approximately zero at $x_{s1} = 0.5$ for the Ca atoms with $(x_{21}+n_{21}, x_{22}+n_{22}, x_{23}+n_{23})$ and $(-x_{21}+n_{21}, -x_{22}+n_{22}, -x_{23}+n_{23})$, and at $x_{s1} = 0.0$ for the Co atoms with $(x_{21}+1/2+n_{21}, x_{22}+1/2+n_{22}, x_{23}+n_{23})$ and $(-x_{21}+1/2+n_{21}, -x_{22}+1/2+n_{22}, -x_{23}+n_{23})$. This takes into account the Ca-defect arrangement in Figures 15 and 16.

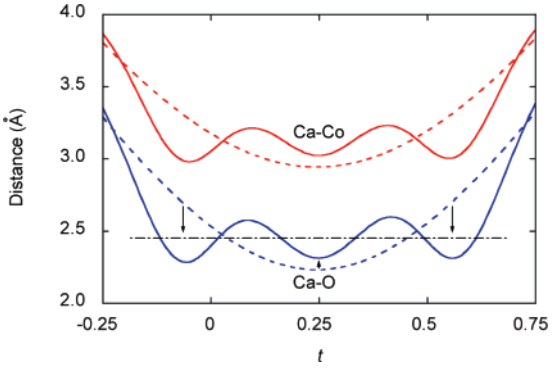

Figure 13. Ca−Co and Ca−O distances plotted as a function of the fourth superspace coordinate t for the average structure (broken lines) and the modulated structure (solid lines) in $(Ca_{0.85}OH)_{2\alpha}CoO_2$ ($\alpha = 0.57822$).

for the first, second, and third NN atoms, respectively. The distances of the first NN atoms are mostly shorter than the value 2.52 Å, estimated from the summation of the effective ionic radii of Ca^{2+} and O^{2-}.[21] This shortened distance suggests that relatively tight intersubsystem chemical bonds are formed between the Ca and the O atoms.

The structural modulation originates in the interaction between the two subsystems. The Ca−O and Ca−Co distance waves are plotted as a function of t in Figure 13. This figure enables us to compare two cases for the average and modulated structures. For the average structure, the Ca−O distance changes monotonously with t. In contrast, for the modulated structure, the Ca−O distance tends to be maintained at a value, ∼2.5 Å, within the wide t range ($-0.1 \leq t \leq 0.6$) by the structure modulation. It suggests that the modulation occurs in order to maintain the appropriate length of the Ca−O bonds in the many parts of the crystal. The Ca−Co distances also exhibit the same tendency. This analysis result indicates that the origin of the modulation arises from the adjustment of the atomic bonding between the subsystems.

Interatomic distances between the OH ions and the O ions modulate, as shown in Figure 10. The modulation amplitude of the first NN OH−O interatomic distances is $2.58 \leq l \leq 3.01$ Å. These values are comparable to the hydrogen-bond distance of OH−O, 2.72 Å. The observed distances are shorter than the typical hydrogen-bond distance, within the range of $0 \leq t \leq 0.35$. This result suggests that the hydrogen bonds are expected to be formed at about 60% (∼0.35/0.57822) of all the OH sites. In Figure 10, the first NN OH−O distance becomes longest, 3.01 Å, at $t = 0.46$. This is due to the above-mentioned "most deformed part", where the hydrogen bonds cannot be formed. It is expected that the role of the hydrogen bonds is atomic bonding between the subsystems, such as the Ca−O bonding. Strong intersubsystem interaction would be formed by the hydrogen bond. More sensitive measurements than powder X-ray diffraction are necessary for detecting the hydrogen bonds precisely. Spectroscopic methods such as Raman scattering, IR-absorption spectroscopy, or NMR could be helpful for this purpose.

It may be of interest to consider the relationship between hole doping into the Co sites and the Ca defect. The arrangement of the hole-doped Co sites and the Ca-defect sites are given in Figure 11. It can be observed that the Ca defects are situated relatively close to the hole-doped Co sites. Figure 14 represents a local structure with atomic coordination around the hole-doped

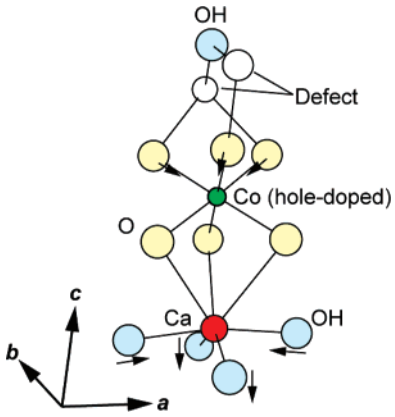

Figure 14. Typical example of the local structure around the hole-doped Co site. The average coordinates of the center Co atom are (6.5, 0.5, 0). The arrows indicate the direction of the deviation from the average position for each atom.

Co atom. The local structure is symmetrical along the a-axis. The Co site is accompanied by a Ca atom directly below the Co atom. Two OH ions adjacent along the a-axis approach the Ca atom. The other two OH ions, adjacent along the b-axis, are significantly driven downward. This is the above-mentioned "most deformed part". The hole-doped CoO_6 octahedron adjoins the "most deformed part", but its effect on the hole doping is not clear. It does not seem to be significant, since the lower three Co−O bond lengths are not significantly affected by the neighboring deformed part.

It is worth noting that the Co site is accompanied also by an OH ion situated directly above the Co atom. The defect sites are situated at both sides of the apical OH ion. The upper three Co−O bond lengths are shortened. This is presumably due to the defect sites, because the upper O ions are free from the Coulombic attractive force of the Ca ions, and the apical OH ion can directly repulse the O ions downward without the Ca ion being an obstacle. Therefore, the upper O ions approach the Co atom, producing the shorter Co−O bonds. As a result, the Co atom holds a high valence state. It seems that hole doping into the Co sites is related to the Ca defects and that the structure reflects this relationship through the modulation.

Concluding Remarks

The modulated structure of a new composite crystal $(Ca_{0.85}OH)_{2\alpha}CoO_2$ ($\alpha \approx 0.57822$) was successfully determined using synchrotron X-ray diffraction data, assuming the superspace group $C2/m(\alpha 10)s0-C2_1/m(\alpha^{-1}10)$. The periodic difference between the $[CoO_2]$ and the $[2Ca_{0.85}OH]$ subsystems causes a displacement of the atoms at all sites. In particular, a unique structural modulation was found in the rock-salt-type $Ca_{0.85}OH$ double atomic layers. It was also found that the Co−O bond lengths are reduced due to the hole doping into the Co sites. The hole doping level and degree of the potential modulation in the CoO_2 conduction layer for $(Ca_{0.85}OH)_{1.16}CoO_2$ are almost the same as in the hole-doped misfit-layer compound, $[Ca_2(Co_{0.65}Cu_{0.35})_2O_4]_{0.63}CoO_2$. The possible arrangement of the hole-doped Co sites and the Ca-defect sites was determined by referring to the bond-valence sum values at the Co sites and the occupation factors at the Ca sites. The local structure around the hole-doped Co site revealed that potential distortion around the Ca-defect sites may cause a reduction of the neighboring Co−O bond lengths to facilitate the introduction of the holes into the Co site.

Acknowledgment. We thank Dr. Yamamoto of NIMS for helpful advice on the crystal structure analysis and specialization of the analysis software, PREMOS2K*i*. We also express sincere thanks to Dr. Nakazawa of NIMS for providing us with the required beam time and the research facilities of BL15XU at SPring-8. We are deeply grateful to Dr. Katsuya of SPring-8 Service Co., Ltd. for his kind technical assistance in the synchrotron X-ray experiments. This research was supported in part by the Superconducting Materials Research Project from the Ministry of Education, Culture, Sports, Science and Technology of Japan, and by the Grants-in-Aid for Scientific Research from the Japan Society for the Promotion of Science (Grant No. 19560686), and by the Iketani Science and Technology Foundation, Tokyo, Japan (Grant No. 0191125-A).

JA072052V